Urban heat island and inertial effects : analyse from field data to spatial analysis

Jérémy Bernard, I. Calmet, E. Bocher, P. Keravec, Marjorie Musy


Jérémy Bernard

Urban heat island and inertial effects : analyse from field data to spatial analysis

Bernard Jérémy[1,2,3], Musy Marjorie[1,2], Calmet Isabelle[1,4], Bocher Erwan[5], Keravec Pascal[1,4]

1 Institut de Recherche en Sciences et Techniques de la Ville, FR CNRS 2488, Ecole Centrale de Nantes - 1 rue de la Noë - BP 92101 – 44321 Nantes - France
2 Centre de Recherche Nantais Architectures Urbanités, UMR CNRS 1563, 6 quai François Mitterrand – BP16202 - 44262 Nantes Cedex 2 - France
3 ADEME, 20 Avenue du Grésillé - 49000 Angers - France
4 Laboratoire de Recherche en Hydrodynamique, Energétique et Environnement Atmosphérique, UMR CNRS 6598, Ecole Centrale de Nantes - 1 rue de la Noë - BP 92101 – 44321 Nantes – France
5 Laboratoire des Sciences et Techniques de l'Information, de la Communication et de la Connaissance – UMR CNRS 6285, Centre de Recherche - BP 92116 - 56321 Lorient - France

dated : 14 June 2015

1. Introduction

The maximum urban heat island (UHI) often occurs few hours after sunset (Oke and Maxwell, 1975) as a consequence of three phenomenons :

- The heat stored by the urban fabric during the day is often higher than the one stored by the rural fabric. This implies that the heat released during the night is also higher in urban areas than in rural areas.
- The long-wave radiation, which is the main flux responsible for cooling during night-time is often limited in urban areas due to low Sky View Factor (SVF).
- The convection, mainly driven by wind velocity and also responsible for cooling during night-time is limited in urban areas due to the high rugosity of its canopy density (Britter and Hanna, 2003)

The combination of those three phenomenons for urban areas results in a lower air cooling rate at the beginning of the night and in a potential time shift of air temperature signal, themselves responsible of the UHI during night-time (UHIn). The UHIn is also weather and season-dependent. When researchers study the UHI effect, they often dissociate seasons and show that the UHI behavior is different from a season to an other (Svensson et al., 2002; Hjort et al., 2011). The influence of cloud covering and wind speed on UHI have also been highlighted by Erell and Williamson (2011) or Svensson et al. (2002) : when cloud covering or wind speed increases, UHI decreases. UHI is defined as a difference of air temperature between an urban area and a rural area. However, air temperature differences are also observed intra urban areas. Geographical context differences (urban form and land-use) have a direct influence on urban energy balance and may explain those differences :

- Groleau and Mestayer (2013) showed that urban albedo values strongly depend on both building and facade density.
- Musy et al. (2012) observed an increase of the Bowen ratio when the percentage of land covered by the vegetation decreases.

The purpose of this study is to show the main factors responsible for air temperature differences intra urban areas during night-time. The correlation between air temperature time shift (Bernabé et al., 2015) and UHIn and cooling rate (Oke and Maxwell, 1975) and UHIn will be investigated under different conditions (time of the year and weather conditions). Ten air temperature stations located in and around the city of Nantes are used to calculate those climatic indicators. Geographical indicators, used to quantify the urban form and the land-use characteristics of the stations surroundings will be built to analyze their correlation with UHIn.

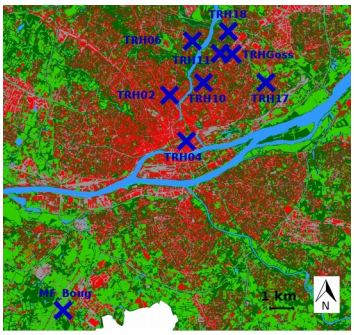

Fig. 1: Study area. Red: buildings, Grey: artificial surfaces, Blue crosses: measurement sites (note that "MF_Nort" is not on the map since it is located at 22 kms on the north of TRH04)

1. Method

1.1 Climatic indicators calculation

Ten measurement stations located in the city of Nantes are used for this study (Fig. 1). Each of them recorded the air temperature every fifteen minutes during

four years (from 2010 to 2014). Further details concerning measurement sites environment and equipment are given in Table 1.

Each climatic indicators is referred to the reference station "MF_Boug", which has the highest accuracy and the lowest uncertainty. They are calculated for each day of the four years. Only days with complete data set (no missing data for all sensors) and no rain fall recorded are conserved for the analysis. Then 305 days are considered for this study. The climatic indicators calculation is described below.

1.1.1 Time shift

The whole day signal is considered for phase shift calculation. Cross-correlation functions $C_{xy}(\tau)$ between a reference station y(t) and each station x(t) are calculated.

The time shift (Δt) between each signal and the reference signal is defined when the cross-correlation function is maximal: $C_{xy}(\Delta t) = C_{xy}^{max}$.

1.1.2 Cooling rate

Oke and Maxwell (1975) showed that the cooling rate (C_r) (air temperature derivative) discriminates an urban site from a rural site mainly during the next few hours following sunset. We chose to calculate the mean C_r of each of our site from sunset to four hours after the sunset.

1.1.3 Night-time urban heat island

Oke and Maxwell (1975) also showed that the cooling rate between an urban and a rural site converge few hours after sunset. When the cooling rate was almost the same, they noticed that the temperature difference between the urban and the rural site was constant and maximum. We chose to calculate this mean difference from four to eight hours after sunset and called it UHIn.

Table 1: Description of the measurement sites and their equipment

Name	Elevation from sea level (m)	Elevation from ground level (m)	Location	Sensor accuracy (K)	Shied		Sampling time (min)
					Ventilation type	Size or type	
TRH02	27	2	Private house – on a wall	+- 0,3	Natural	cylindric (85 x 90 mm³) – 9 plates	15
TRH04	8	4,5	Private house – on a wall	+- 0,3	Natural	cylindric (85 x 90 mm³) – 9 plates	15
TRH06	27	2	Engineer school – on a pole	+- 0,3	Natural	cylindric (85 x 90 mm³) – 9 plates	15
TRH10	24	5	Private house – on a wall	+- 0,3	Natural	cylindric (85 x 90 mm³) – 9 plates	15
TRH11	22	2,5	Administration building – on a wall	+- 0,3	Natural	cylindric (85 x 90 mm³) – 9 plates	15
TRH17	13	3	Administration building – on a pole surrounded by trees	+- 0,3	Natural	cylindric (85 x 90 mm³) – 9 plates	15
TRH18	25	2	Administration building – on a wall	+- 0,3	Natural	cylindric (85 x 90 mm³) – 9 plates	15
Goss	29	1,8	Open field – on a pole	+- 0,15	Natural	EE21 shield[1]	Averaged every 15 minutes
MF_Boug	26	1,5	Open field – on a "tripod"	+-0,1	Natural	Socrima® "*petit modèle*"[2]	60 – linear interpolated every 15 minutes
MF_Nort_s_e	13	1,5	Open field – on a "tripod"	Unknown	Natural	Socrima® "*petit modèle*"[2]	60 – linear interpolated every 15 minutes

1.2 Seasonal and weather classification

The influence of both the season and the weather conditions (wind speed and nebulosity) on the climatic indicators value is analyzed.

Urban climatic behavior is different according to the period of the year. Thus climatic indicators results are sorted by season. Month could be a more interesting time scale but the data amount is not big enough to conserve a sufficient number of days representative of each month.

Wind speed and nebulosity are two key parameters to analyze UHI values (Erell and Williamson, 2011 ; Svensson et al., 2002). They are recorded every hours at the reference station. The wind speed sensor, which is located at 10 m above the ground, is a 2-dimension ultrasonic anenometer (Alizia Pulsonic[3]). The nebulosity is evaluated by human observation. Both the wind speed and the nebulosity are averaged during a different period

[1]http://www.epluse.com/fileadmin/data/product/ee21/datasheet_EE21.pdf
[2]http://education.meteofrance.fr/ressources-pour-les-enseignants/observer-et-mesurer/l-abri-meteo#
[3]http://www.pulsonic.net/ultrasonic-anemometer-alizia-380/id-menu-219.html

of the day depending on the climatic indicator which is considered (all day for Δt, from sunset to four hours after sunset for C_r and from four to eight hours after sunset for UHIn).

A preliminary study is performed to sort wind speed and nebulosity in different categories regarding the effect of the value they take on the climatic indicators value. The results of this classification are given in paragraph 2.

1.3 Geographical indicators calculation

The urban form and the land-use type surrounding the sensor play a major role on the measured air temperature. The size and the shape of the area to consider for geographical indicator calculation are key factors when relationships between geographical and climatic indicators are investigated. Two main approaches are traditionally used. The first approach consist in an a priori partitioning of the territory based on :

- A regular grid with a specific mesh shape (square, triangular, etc.) ;
- The road network : each mesh resulting is called "city block" (Lesbegueries et al., 2009) ;
- Homogeneous Local Climate Zones (LCZ) which can be designed according to specific geographical and climatic parameters (Lelovics et al., 2014).

The second approach is to consider a buffer circle around each station as the reference surface for geographical indicator calculation. The size of the circle may be the same for each station or be dependent on the urban form of the close surrounding. Usually, higher is the building density, smaller the buffer circle. This method is mainly used when the stations location has been decided arbitrarily (without using a preliminary partitioning), which is the case for our stations. This second approach will be used for this study, using an arbitrary radius of 100 m for each station, which is the minimum size usually found in the litterature (Chen et al., 2012).

Two main databases are used for geographical indicator calculation :

- BDTopo® for buildings informations (height, shape) and water surfaces[4].
- Land use data produced from remote sensing images (SPOT – 2,5 m of spatial resolution) to locate artificial surfaces, bare ground and high and low vegetation areas (Long et al., 2014).

The geographical indicators produced thanks to those databases from OrbisGIS platform (Bocher and Petit, 2012) are given in Table 2.

Table 2: Implemented geographical indicators

Symbol	Name	Formula	Useful inputs
H	Average building height	$\frac{\sum_i h_i a_i}{\sum_i a_i}$	A_{ref} : buffer circle area (m²)
D_{Flin}	Linear of facade density	$\frac{\sum_i p_i}{A_{ref}}$	a_{b_i} : area taken by the building i
OSR	Open space area	$1-\frac{\sum_i a_i}{A_{ref}}$	h_i : height of the building i
D_{VB}	Building volume density	$\frac{\sum_i h_i a_i}{A_{ref}}$	p_i : perimeter of the building i
D_F	Facade density	$\frac{\sum_i p_i h_i}{\sum_i p_i h_i + A_{ref}}$	a_{vh_i} : area taken by the high vegetation i
D_{veg}	Vegetation density	$\frac{\sum_i a_{vli} + \sum_i a_{vhi}}{A_{ref}}$	a_{vl_i} : area taken by the low vegetation i
ADM	Equivalent admittance	$\mu_a \cdot (D_{Flin} \cdot h_w + \frac{a_{ai}}{A_{ref}}) + \mu_{vh} \cdot \frac{a_{vhi}}{A_{ref}} + \mu_{vl} \cdot \frac{a_{vli}}{A_{ref}}$	a_{bg_i} : area taken by the bare ground i
			a_{a_i} : area taken by the artificial surface i
			μ_a = 700, μ_{vl} = 175, μ_{vh} = 350 : thermal admittance for artificial surfaces, low vegetation and high vegetation ($J.m^{-2}.s^{-1/2}.K^{-1}$)
			h_w = 3 : wall height to consider as influent on the air temperature at screen height

2. Results

The climatic indicator the more impacted by the wind speed and the nebulosity values is UHIn, as shown in Fig. 2 for autumn time (season containing a big range of both wind speed and nebulosity values). The season affects the maximum value of UHIn but does not affect the shape of those two curves.

[4] http://professionnels.ign.fr/bdtopo.

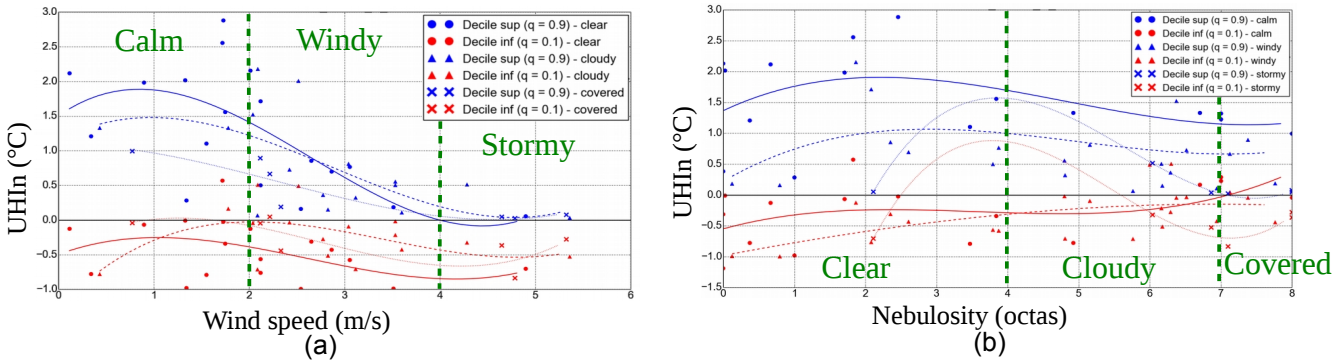

Fig. 2: Variation of UHIn during autumn time with (a) wind speed and (b) nebulosity

As a result of this analysis, three types of conditions are defined for each climatic variable (green dashed line Fig. 2). This classification will be used for the following study.

Simple linear regressions are performed between each of the three climatic indicators under different seasonal and weather conditions. The offset is set to zero since the regression line should pass through the values taken by the reference station (which is zero for every climatic indicator). Some typical examples of result are given Fig. 3. Slopes and determination coefficient are given for all cases in Table 3, as well as the number of days used for each analysis.

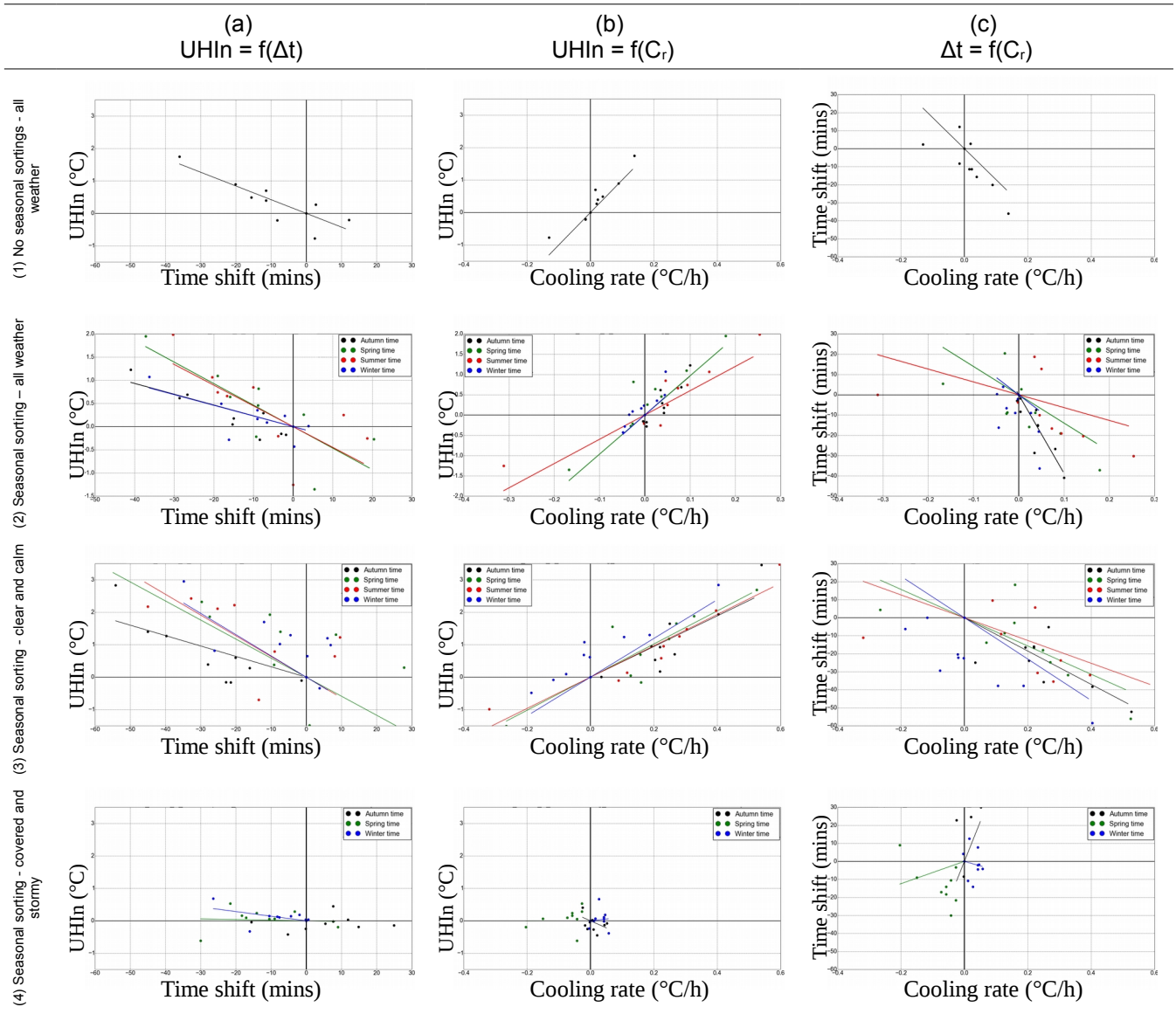

Fig. 3: Linear regressions between climatic indicators under different seasons and weather conditions

Table 3: Resulting parameters of linear regressions performed between climatic indicators under different seasons and weather conditions. Bold: results considered for the analysis (R^2 > 0,5 and day number > 5)

Season / weather conditions	Parameters	(a) UHIn = f(Δt) Summer	Spring	Autumn	Winter	(b) UHIn = f(C_r) Summer	Spring	Autumn	Winter	(c) Δt = f(C_r) Summer	Spring	Autumn	Winter
(1) No seasonal sortings - all weather	Slope	**-0,042**				**10**				**-170**			
	R^2	**0,79**				**0,86**				**0,57**			
	Day number	**305**				**305**				**305**			
(2) Seasonal sorting - all weather	Slope	**-0,045**	**-0,046**	**-0,023**	**-0,023**	**6,0**	**9,7**	**9,6**	**9,9**	*-63*	**-140**	**-390**	*-170*
	R^2	**0,61**	**0,70**	**0,79**	**0,60**	**0,84**	**0,82**	**0,80**	**0,58**	*0,31*	**0,53**	**0,90**	*0,15*
	Day number	**94**	**94**	**45**	**72**	**94**	**94**	**45**	**72**	*94*	**94**	**45**	*72*
(3) Seasonal sorting - clear and calm	Slope	**-0,064**	**-0,059**	**-0,032**	*-0,066*	**4,8**	**5,1**	**4,7**	**6,0**	**-63**	**-78**	**-93**	*-115*
	R^2	**0,74**	**0,62**	**0,75**	*0,53*	**0,94**	**0,85**	**0,90**	**0,69**	**0,62**	**0,71**	**0,86**	*0,40*
	Day number	**11**	**6**	**8**	*3*	**19**	**16**	**9**	**8**	**19**	**16**	**9**	*8*
(4) Seasonal sorting - covered and stormy	Slope	-	*-0,0019*	*~ 0*	*-0,014*	-	*~ 0*	*-4,3*	*1,1*	-	*62*	*440*	*-50*
	R^2	-	*0,011*	*~ 0*	*0,36*	-	*~ 0*	*0,21*	*0,020*	-	*0,13*	*0,11*	*0,051*
	Day number	*0*	*1*	*3*	*5*	*0*	*1*	*3*	*5*	*0*	*1*	*2*	*5*

Relationships between climatic and geographical indicators are established under each seasonal and weather conditions. High determination coefficient is met mainly when the sky is clear or cloudy and wind speed is calm or windy. D_{Flin} is one of the most explanative indicator for each climatic indicator. ADM, which was expected to make D_{Flin} more consistent (according to Bernabé et al. (2015)) explains even better the climatic indicators.

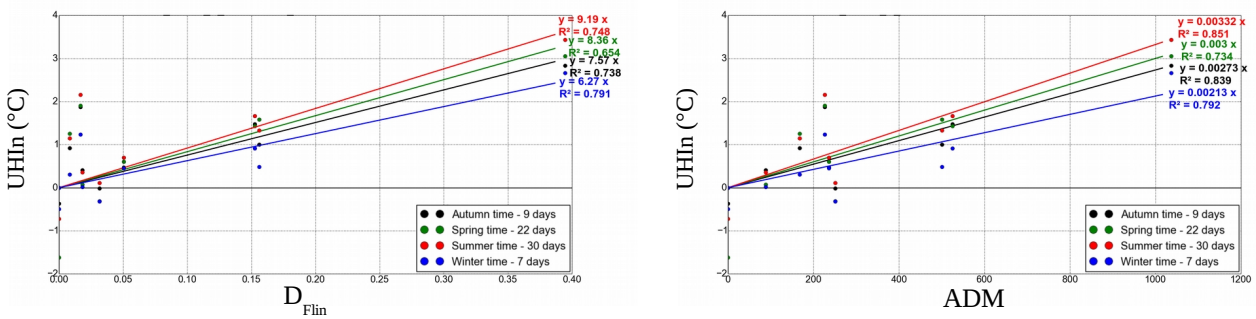

(a) (b)

Fig. 4: Linear regression under clear and calm conditions between (a) UHIn and D_{Flin} and (b) UHIn and ADM

3. Discussions

The wind speed value seems to be more influent on the UHIn than the nebulosity (Fig. 2). UHIn value is really affected by the wind when its speed exceed 3 m/s, observation consistent with previous studies (Svensson et al, 2002; Erell and Williamson, 2007). Under 5 - 6 octas, nebulosity does not affect much the UHIn (even for summer season), threshold being often lower (around 2 – 3 octas) when compared to similar studies.

The results of the Table 3 which will be considered for the analysis are only those which have R^2 > 0,5 and day number > 5. We first see that it is hard to find relationships between our climatic indicators during winter time, either because of a low number of clear and calm day, or maybe because other process not taken into account in this study are responsible of the values taken by our climatic indicators. Time shift and cooling rate explain well the UHIn for the other seasons. Clear and calm conditions are favourable to discriminate our ten stations : the indicators range is indeed much smaller under covered and stormy conditions (Fig. 3). Seasons and weather conditions also have an influence on the slope of the linear regression line : it decreases between winter-time and summer-time for cases (a) and (b) whereas it increases for case (c). The same behaviour is noticed when the weather is clearer and calmer. This means that our climatic indicators are not affected in the same way by season or weather variation. Cooling rate is the most sensitive to season or weather variation, followed by the phase shift and then UHIn. The autumn and spring cooling rate seems the climatic indicator the most affected by the clear and calm day filtering. The slopes for cases (b) and (c) are indeed almost divided by two. Autumn and spring are maybe favourable to high number of cloudy and stormy or covered and windy days, which directly affect the

slopes of (b)(2) and (c)(2). The UHIn is almost 100 % determined by the cooling rate when the weather conditions are clear and calm. It means that under those conditions, the four hours following the sunset are essential in the UHIn formation. A sensitivity analysis could be performed to better evaluate which hours contribute the most to UHIn formation.

UHIn is well determined by D_{Flin} and ADM under clear and calm conditions, whatever be the season. Those relationships might be used to determine the night-time hottest areas of the Nantes conurbation during heat waves. Heat waves are indeed characterized by clear and calm conditions and the night-time temperature is a key parameter to measure health risk for people (Clarke and Bach, 1971 ; Besancenot, 2002). Nevertheless, geographical indicators values taken by our ten stations are not equally distributed, especially D_{flin}. Only one station (TRH04) has a high D_{Flin} and ADM, which may then distort the regression model.

Overall, the following improvements are suggested to confirm our results :

- The thresholds for weather conditions classification should be set according to a more quantitative approach than the one used for this study.
- The number of measurement sites is currently too low to perform good regression analysis. Eleven new sites have been equipped in 2015, which will allow to verify the veracity of the results obtained in this study. Moreover, those new sensors have been set on poles rather than walls to improve measurement representativeness (Oke, 2004).
- The size and the shape of the elementary areas defined for geographical analysis have been chosen arbitrarily. A comparative analysis using several territory partitioning methods might be performed in order to identify the one which gives the best results..

Acknowledgment

This work was supported by the French Environment and Energy Management Agency (ADEME), AgroCampus Ouest (ACO) and Region des Pays de la Loire. The authors wish to thank the OrbisGIS team for their technical support and advices: http://www.orbisgis.org/about/the-team/ as well as Meteo-France for the availability of their measurement data.

References

Bernabé, A., Bernard, J., Musy, M., Andrieu, H., Bocher, E., Calmet, I., ... & Rosant, J. M. (2015). Radiative and heat storage properties of the urban fabric derived from analysis of surface forms. *urban climate*, ***12***, 205-218.Britter, R. E., & Hanna, S. R., 2003. Flow and dispersion in urban areas. *Annual Review of Fluid Mechanics*, ***35*****(1)**, 469-496.

Besancenot, J. P., 2002. Vagues de chaleur et mortalité dans les grandes agglomérations urbaines. *Environnement, risques & santé*, ***1*****(4)**, 229-40.

Bocher, E., Petit, G., 2012. OrbisGIS: Geographical Information System designed by and for research. In: Bucher, B., Le Ber, F., (Ed.), Innovative Software Development in GIS, ISTE & Wiley, Geographical Information System series, pp. 25–66.

Britter, R. E., & Hanna, S. R. (2003). Flow and dispersion in urban areas. *Annual Review of Fluid Mechanics*, ***35*****(1)**, 469-496.

Chen, L., Ng, E., An, X., Ren, C., Lee, M., Wang, U., & He, Z. (2012). Sky view factor analysis of street canyons and its implications for daytime intra-urban air temperature differentials in high-rise, high-density urban areas of Hong Kong: a GIS-based simulation approach. *International Journal of Climatology*, ***32*****(1)**, 121-136.

Clarke, J. F., & Bach, W., 1971. Comparison of the comfort conditions in different urban and suburban microenvironments. *International journal of biometeorology*, ***15*****(1)**, 41-54.

Erell, E., & Williamson, T., 2007. Intra-urban differences in canopy layer air temperature at a mid-latitude city. *International Journal of Climatology*, ***27*****(9)**, 1243-1256.

Groleau, D., Mestayer, P.G., 2013. Urban morphology influence on urban albedo: a revisit with the solene model. Boundary-Layer Meteorol. **147 (2)**, 301–327.

Hjort, J., Suomi, J., & Käyhkö, J., 2011. Spatial prediction of urban–rural temperatures using statistical methods. *Theoretical and applied climatology*, ***106*****(1-2)**, 139-152.

Lelovics, E., Unger, J., & Gál, T., 2014. Design of an urban monitoring network based on local climate zone mapping and temperature pattern modelling. *Climate Research*, ***60***, 51-62.

Lesbegueries, J., Lachiche, N., Braud, A., Skupinski, G., Puissant, A., Perret, J., 2009. A platform for Spatial Data Labeling in an Urban Context. In: Presentation at the International Opensource Geospatial Research Symposium 2009 – OGRS09.

Long, N., Bellec, A., Bocher, E., Petit, G., 2014. Influence of the methodology (pixel-based vs object-based) to extract urban vegetation from VHR images in different urban zones. In: 5th Presentation at the Geobia Conference.

Musy, M., Gutleben C., Inard C., Long N., Mestayer P., Rodriguez F., Rosant, J.M., 2012. VegDUD project: role of vegetation in sustainable urban development. In: Presentation at the 8th International Conference on Urban Climate and 10th Symposium on the Urban Environment. Dublin.

Oke, T. R., & Maxwell, G. B., 1975. Urban heat island dynamics in Montreal and Vancouver. *Atmospheric Environment (1967)*, ***9*****(2)**, 191-200.

Oke, T. R., 2004. *Initial guidance to obtain representative meteorological observations at urban sites*, **Vol. 81**. Geneva: World Meteorological Organization.

Svensson, M. K., Eliasson, I., & Holmer, B., 2002. A GIS based empirical model to simulate air temperature variations in the Goteborg urban area during the night. *Climate Research*, ***22*****(3)**, 215-226.